ACS Medicinal Chemistry Letters

Letter

pubs.acs.org/acsmedchemlett

Discovery of Potent and Orally Active p53-MDM2 Inhibitors RO5353 and RO2468 for Potential Clinical Development

Zhuming Zhang,*[,†,⊥] Xin-Jie Chu,*[,†,⊥] Jin-Jun Liu,[†] Qingjie Ding,[†] Jing Zhang,[†] David Bartkovitz,[†] Nan Jiang,[†] Prabha Karnachi,[†] Sung-Sau So,[†] Christian Tovar,[§] Zoran M. Filipovic,[§] Brian Higgins,[§] Kelli Glenn,[∥] Kathryn Packman,[§] Lyubomir Vassilev,[§] and Bradford Graves[‡]

[†]Discovery Chemistry, [‡]Discovery Technologies, [§]Discovery Oncology, and [∥]Non-Clinical Development, Roche Pharma Research, Hoffmann-La Roche, Inc., 340 Kingsland Street, Nutley, New Jersey 07110, United States

Supporting Information

ABSTRACT: The development of small-molecule MDM2 inhibitors to restore dysfunctional p53 activities represents a novel approach for cancer treatment. In a previous communication, the efforts leading to the identification of a non-imidazoline MDM2 inhibitor, RG7388, was disclosed and revealed the desirable in vitro and in vivo pharmacological properties that this class of pyrrolidine-based inhibitors possesses. Given this richness and the critical need for a wide variety of chemical structures to ensure success in the clinic, research was expanded to evaluate additional derivatives. Here we report two new potent, selective, and orally active p53-MDM2 antagonists, RO5353 and RO2468, as follow-ups with promising potential for clinical development.

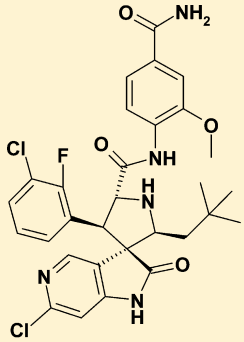

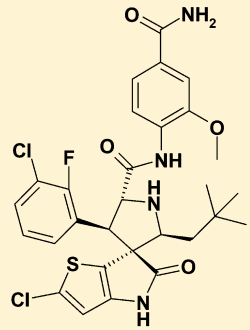

KEYWORDS: *MDM2, p53, wild-type, small molecule, apoptosis, cancer*

Tumor suppressor p53 is a potent transcription factor that is activated in response to cellular stress and regulates downstream genes controlling cell cycle arrest and apoptosis.[1−4] Dysfunction of the p53 pathway is the most frequent alteration observed in human cancers.[5] MDM2 is the primary negative regulator of p53 through binding to its transactivation domain and promoting proteosomal degradation.[6−8] In tumor cells with wild-type p53 (∼50%), reactivation of the p53 pathway by inhibition of MDM2 with small molecules has been considered as potentially an attractive novel therapeutic approach for cancer treatment.[9,10] Currently, several small-molecule MDM2 inhibitors including RG7112 and RG7388 (Figure 1) are undergoing clinical evaluations.[11−14] To maximize the chance of success in the clinic and derisk any potential idiopathic toxicity associated with specific chemotypes, continued research efforts are required to expand chemodiversity and identify potent and selective MDM2 antagonists with desirable in vitro ADMET and in vivo pharmacokinetic properties. Here we report the discovery of RO5353 and RO2468, two new highly potent and selective MDM2 inhibitors with potential for clinical development.

Our exploration initially led to the identification of a potent and selective MDM2 inhibitor RO8994 (Figure 1), which was found to be highly efficacious against established human tumor xenografts in nude mouse models.[15] Two key structural elements of RG7388 were preserved in RO8994. First, it was established that the stereochemical configuration of the pyrrolidine core structure in which the two aryl rings ("A" and "B") adopt a "*Trans*" orientation was very important for optimal binding to MDM2.[14] The architecture of spiroindolinone-3,3′-pyrrolidine series (as exemplified by MI-219) was first reported by Ding et al.[16−18] Consistent with our findings, this group recently published their latest findings in which the original stereochemistry was found to be unstable and

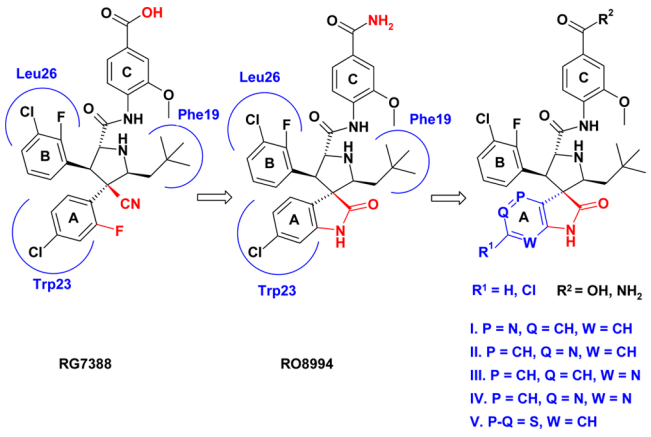

Figure 1. Chemical structures of RG7388, RO8994, and analogues I−V. Binding modes for RG7388 and RO8994 are shown.

Received: September 13, 2013
Accepted: December 29, 2013
Published: December 29, 2013

converted over time to the more stable "*Trans*" configuration as shown in RO8994.[19] Second, a methoxy *para*-benzoic acid moiety in RG7388 ("C" in Figure 1) was transferred to RO8994, in which a slight modification was made by converting the terminal carboxylic acid to a carboxamide moiety. In contrast to aliphatic groups,[19,20] the aromatic group ("C") proved to be critical for both RG7388 and RO8994 as it stabilized the molecule metabolically, significantly improved cellular potency/selectivity, PK profiles, and in vivo efficacy.[14,15]

On the basis of the crystal structures, the 3-chloro-2-fluorophenyl group binds to the Leu26 pocket on MDM2, while the neopentyl group occupies the Phe19 pocket (Figure 1).[14,15] As expected from the binding models with the Michigan oxindole compounds,[16] the 6-chloroxindole moiety in RO8994 is buried into the deep, narrow Trp23 pocket, and its NH moiety forms a hydrogen bond with a backbone carbonyl of MDM2 for enhanced binding affinity.[15] Since the interaction in the Trp23 pocket appears to be the most critical, further exploration of bioisosteric replacements on the phenyl moiety of 6-chlorooxindole, while preserving other important architectural features in RO8994 for optimal binding and pharmacological properties, was prioritized.[21] Thus, we describe our work in detail on selected analogues of 4-, 5-, and 7-azaoxindole (I–III), 2-chloropyrrolo[2,3-d]pyrimidin-6-one (IV), and 2-chlorothienyl[3,2-b]pyrrol-5-one (V) (Figure 1).

Recently a practical synthesis of RO8994 has been established.[22] Utilizing these new methods, azaoxindole, 2-chloropyrrolo[2,3-d]pyrimidin-6-one, and 2-chlorothienyl [3,2-b]pyrrol-5-one analogues in I–V were efficiently synthesized as outlined in Scheme 1. The key step is the cycloaddition reaction of VI with common intermediate VII catalyzed by lithium hydroxide to form thermodynamically more stable stereochemical isomer as shown in the structure VIII.[15,22] Other regio- or stereochemical isomers of compound VIII were also formed but could be readily separated by chromatography.

Scheme 1. Racemic Synthesis of Azaoxindole I–III, 2-Chloropyrrolo[2,3-b]pyrimidin-6-one IV, and 2-Chlorothienyl[3,2-b]pyrrol-5-one V Analogues[a]

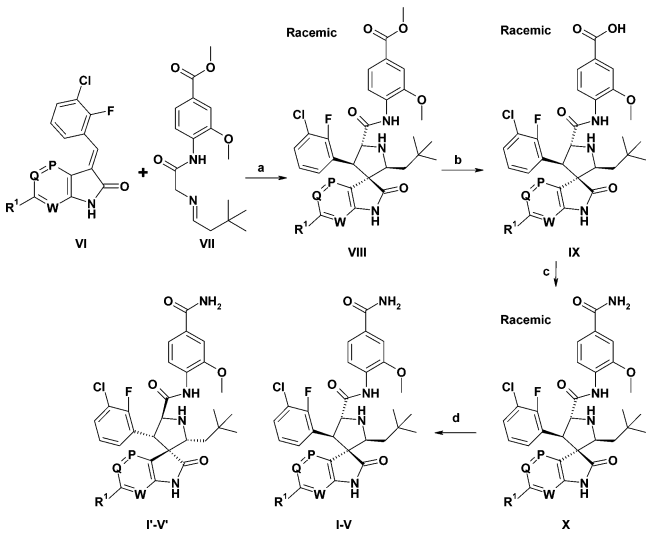

[a]Reagents and conditions: (a) LiOH, THF, 40 °C; (b) LiOH, THF, H_2O, rt; (c) CDI, NH_4OH, THF, rt; (d) chiral SFC separation; P, Q, and W as defined in Figure 1.

To quickly assess the effects of bioisosteric replacements in scaffolds I–V (Figure 1), compounds **1**–**13** were prepared initially as racemic mixtures of two enantiomers (Figure 2). All

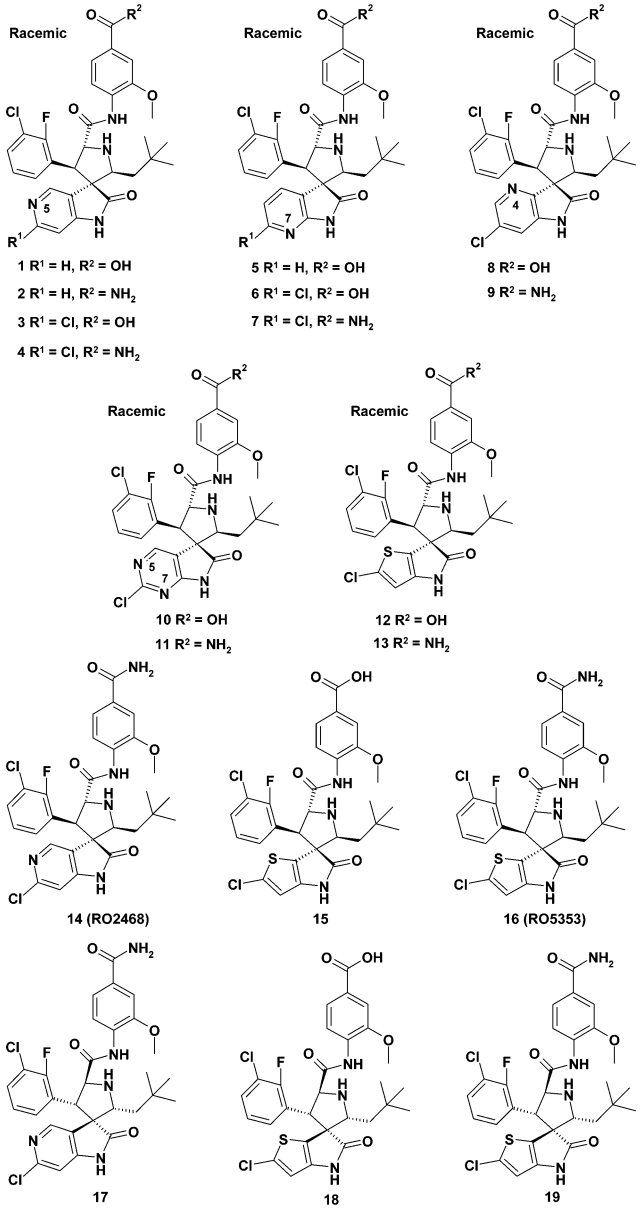

Figure 2. Chemical structures of analogues **1**–**19** in I–V.

analogues display potent biochemical affinity with IC_{50} values <100 nM in the binding assay (Table 1). In cellular antiproliferative MTT assays, their potencies against wild-type p53 cell line SJSA vary over a wide range from IC_{50} = 22.7 to 0.009 μM, but all appear to be selective against a mutant p53 cell line, SW480. Lack of the chloro substituent at the R^1 position (compounds **1**, **2**, and **5**) clearly led to weaker binding affinity in the binding assay and significant loss in cellular potency against SJSA compared to corresponding compounds with R^1 = Cl (**3**, **4**, and **6**). The antiproliferative potencies (Table 1) of compounds **6**, **7**, **10**, and **11** against SJSA are generally slightly weaker compared to analogues **3**, **4**, **8**, and **9**, indicating the placement of heteroatom N at position 7 as shown in scaffolds III and IV is not favorable. Nevertheless, compounds **4**, **12**, and **13** as racemic mixtures were found to

dx.doi.org/10.1021/ml400359z | ACS Med. Chem. Lett. 2014, 5, 124–127

Table 1. Activity Results for Analogues 1−13 and RO8994 in a Biochemical Binding Assay and Human Cancer Cell Proliferation Assays[a]

compd	1	2	3	4	5	6	7	8	9	10	11	12	13	RO8994
HTRF IC_{50} (nM)[b]	52	140	47	17	52	18	11	46	52	25	45	33	40	5
SJSA IC_{50} (μM)[c]	22.7	2.11	0.043	0.014	1.37	0.045	0.067	0.061	0.042	0.10	0.09	0.009	0.011	0.013
SW480 IC_{50} (μM)[d]	>30	13.4	>30	12.8	>30	15.4	5.26	>30	5.9	>30	10.7	29.3	7.87	5.19

[a]IC_{50} was determined by one experiment performed in duplicate. [b]0.2% BSA in the buffer. [c]Wild-type p53 cancer cell line. [d]Mutant p53 cancer cell line.

display cellular potency and selectivity comparable to RO8994. These compounds were separated into chiral enantiomers **14**−**19** by chiral super fluid chromatography (SFC) (Figure 2).

The potent activity of **4**, **12**, and **13** was confirmed by assessment of their enantiomers **14**, **15**, and **16** (Tables 2 and 3). In the binding assay, **14** (IC_{50} = 6 nM) is 960-fold more potent than its enantiomer **17** (Table 2). In contrast, **15** (IC_{50} = 7 nM) and **16** (IC_{50} = 6 nM) are only 8- and 30-fold more potent than their enantiomers **18** and **19**. In antiproliferative assays (Table 3), **14, 15**, and **16** display high potency against a panel of wild-type p53 cancer cell lines (SJSA, HCT116, and RKO) and high selectivity relative to mutant cell lines (SW480 and MDA-MB-435). Compounds **18** and **19** displayed moderate cellular activity with much less selectivity (Table 3). Absolute stereochemical configuration of the more active enantiomers **15** and **16** were confirmed by a crystal structure of **16** bound to MDM2 (Figure 3).

Table 2. Affinity of Analogues 14−19 and RO8994 in a Biochemical Binding Assay[a]

compd	14	15	16	17	18	19	RO8994
HTRF IC_{50} (nM)	6	7	7	5764	57	177	5

[a]IC_{50} was determined by one experiment performed in duplicate.

Table 3. Antiproliferative Activity of Analogues 14-19 in Human Cancer Cell lines[a]

compd	14	15	16	18	19	RO8994
MTT IC_{50} (μM)[b]	0.015	0.003	0.007	0.18	0.85	0.02
selectivity[c]	742	5300	1023	88	8	312

[a]IC_{50} was determined by one experiment performed in duplicate. [b]Average IC_{50} of three wt-p53 cancer cell lines (SJSA, HCT116, and RKO). [c]Ratio of average IC_{50} of two mutant p53 cell lines (SW480 and MDA-MB-435) and average IC_{50} of three wild-type p53 cell lines (same as above).

Since compounds **14**, **15**, and **16** exhibit substantial cellular antiproliferative potency/selectivity and compare favorably to RO8994, these analogues were evaluated for their in vivo pharmacokinectic characteristics. Compound **15** displays low plasma exposure orally and a high clearance rate in mice. In contrast, both compounds **14** and **16** demonstrate excellent PK profiles (Table 4). Both **14** (RO2468) and **16** (RO5353) achieve impressive in vivo efficacy against established human SJSA1 osteosarcoma xenoftrafts in nude mice (Figures 4 and 5) at doses and exposures comparable to RO8994. Both **14** and **16** displayed tumor regression at 10 mg/kg. In a similar study, RO8994 exhibited regression at 6.25 mg/kg.[15] No significant weight loss was observed, consistent with the nongenotoxic p53 activation mechanism.

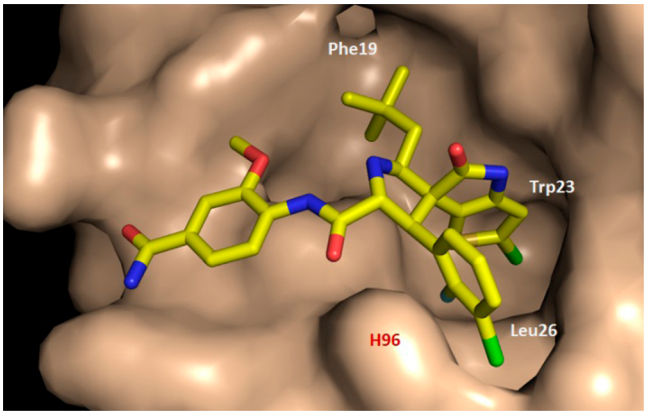

Figure 3. Crystal structure of **16** bound to MDM2. The 2-chlorothienyl[3,2-b]pyrrol-5-one group is buried in the Trp23 pocket. The 3-chloro-2-fluorophenyl group occupies the Leu26 pocket. This structure is available at the PDB (code 4LWV).

Table 4. Human Liver Microsomal Stability and Mean Single Dose PK Parameters of Compounds 14, 15, and 16 and RO8994 in C57 Male Mice by Oral and IV Dosing

compd	14	15	16	RO8994
HLM_CL (mL/min/kg)[a]	10.2		2.0	7.5
PO dose (mg/kg)	5	10	10	25
PO AUC/dose (μg·hr/mL/mg/kg)	4.2	0.08	1.5	3.7
PO C_{max} (μg/mL)	2.1	0.3	1.3	5.8
IV dose (mg/kg)	2	2.5	2.5	0.64
CL (mL/min/kg)	1.8	68.6	9.9	5.8
$t_{1/2}$ (h)	3.0	1.68	3.0	7.1
F (%)[b]	46	32	92	92

[a]For HLM_CL: low clearance < 6.5; 6.5 < medium clearance < 35; high clearance > 35. [b]Oral bioavailability.

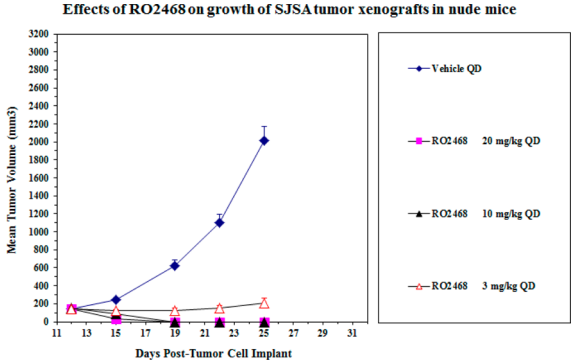

Figure 4. Oral in vivo efficacy profile of **14** (RO2468) on nude mice implanted with SJSA1 osteosarcoma. Tumor stasis was observed at 3 mg/kg QD and tumor regression was observed at 10 mg/kg QD.

dx.doi.org/10.1021/ml400359z | ACS Med. Chem. Lett. 2014, 5, 124−127

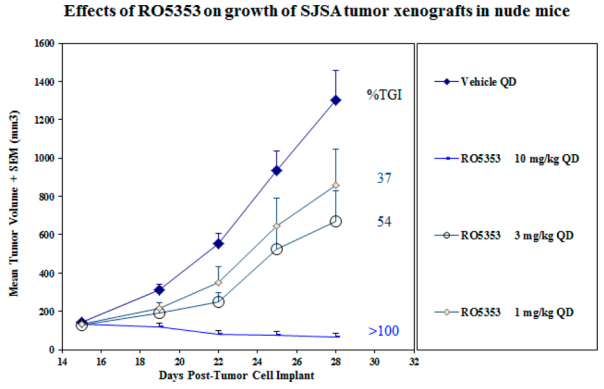

Figure 5. Oral in vivo efficacy profile of **16** (RO5353) on nude mice implanted with SJSA1 osteosarcoma. Significant tumor growth inhibition was observed at 3 mg/kg QD and tumor regression was observed at 10 mg/kg QD.

In summary, our investigation of bioisosteric replacements of the 6-chlorooxindole group in RO8994 led to the identification of two highly potent, selective, and orally active p53-MDM2 inhibitors, RO2468 or RO5353, with promising potential for clinical development.

■ ASSOCIATED CONTENT

Supporting Information

Detailed experimental section, including X-ray crystal data of **16**. Detailed results in HTRF biochemical binding affinity, MTT cellular antiproliferative assays, human liver microsomal stability, and in vivo animal model. This material is available free of charge via the Internet at http://pubs.acs.org.

■ AUTHOR INFORMATION

Corresponding Authors

*(Z.Z.) Phone: (215) 628-7076. E-mail: zzzhang_3000@yahoo.com.

*(X.-J.C.) E-mail: xinjiechu@gmail.com.

Author Contributions

⊥Z.Z. and X.-J.C. contributed equally to this work.

Notes

The authors declare no competing financial interest.

■ ACKNOWLEDGMENTS

SFC purification by Theodore Lambros, detailed ^{1}H and NOE NMR analysis for determination of stereochemical configuration by Gino Sasso, and high-resolution mass by George Perkins are greatly acknowledged.

■ REFERENCES

(1) Harris, S. L.; Levine, A. J. The p53 pathway: positive and negative feedback loops. *Oncogene* **2005**, *24* (17), 2899−2908.

(2) Michael, D.; Oren, M. The p53-MDM2 module and the ubiquitin system. *Semin. Cancer Biol.* **2003**, 49−58.

(3) Levine, A. J. The cellular gatekeeper for growth and division. *Cell* **1997**, *88*, 323−331.

(4) Vogelstein, B.; Lane, D.; Levine, A. J. Surfing the p53 network. *Nature* **2000**, *408*, 307−310.

(5) Hainaut, P.; Hollstein, M. p53 and human cancer: the first ten thousand mutations. *Adv. Cancer Res.* **2000**, *77*, 81−137.

(6) Bond, G. L.; Hu, W.; Levine, A. J. MDM2 is a central node in the p53 pathway: 12 years and counting. *Curr. Cancer Drug Targets* **2005**, *5*, 3−8.

(7) Freedman, D. A.; Wu, L.; Levine, A. J. Functions of the MDM2 oncoprotein. *Cell. Mol. Life Sci.* **1999**, *55*, 96−107.

(8) Momand, J.; Zambetti, G. P.; Olson, D. C.; George, D.; Levine, A. J. The mdm-2 oncogene product forms a complex with the p53 protein and inhibits p53-mediated transactivation. *Cell* **1992**, *69*, 1237−1245.

(9) Brown, C. J.; Lain, S.; Verma, C. S.; Fersht, A. R.; Lane, D. P. Awakening guardian angels: drugging the p53 pathway. *Nat. Rev. Cancer* **2009**, *9*, 862−873.

(10) Vassilev, L. T. MDM2 inhibitors for cancer therapy. *Trends Mol. Med.* **2007**, *13*, 23−31.

(11) Ray-Coquard, I.; Blay, J. Y.; Italiano, A.; Le Cesne, A.; Penel, N.; Zhi, J.; Heil, F.; Rueger, R.; Graves, B.; Ding, M.; Geho, D.; Middleton, S. A.; Vassilev, L. T.; Nichols, G. L.; Bui, B. N. Effect of the MDM2 antagonist RG7112 on the P53 pathway in patients with MDM2-amplified, well-differentiated or dedifferentiated liposarcoma: an exploratory proof-of-mechanism study. *Lancet Oncol.* **2012**, *13* (11), 1133−1140.

(12) Carry, J.-C.; Garcia-Echeverria, C. Inhibitors of the p53/hdm2 protein-protein interaction-path to the clinic. *Bioorg. Med. Chem. Lett.* **2013**, *23*, 2480−2485.

(13) Ma, Y.; Lahue, B. R.; Shipps, G. W.; Wang, Y.; Bogen, S. L.; Voss, M. E.; Nair, L. G.; Tian, Y.; Doll, R. J.; Guo, Z.; Strickland, C. O.; Zhang, R.; McCoy, M. A.; Pan, W.; Siegel, E. M.; Gibeau, C. R. Substituted Piperidines that Increase p53 Activity and the Uses Thereof. *U.S. Pat. Appl. Publ.* US 20080004287 A1, 2008.

(14) Ding, Q.; Zhang, Z.; Liu, J.-J.; Jiang, N.; Ross, T. M.; Chu, X.-J.; Bartkovitz, D.; Podlaski, F. J.; Janson, C.; Tovar, C.; Filipovic, Z. M.; Higgins, B.; Glenn, K.; Packman, K.; Vassilev, L.; Graves, B. Discovery of RG7388, a potent and selective p53-MDM2 inhibitor in clinical development. *J. Med. Chem.* **2013**, *56* (14), 5979−5983.

(15) The detailed analyses on SAR development and in vitro and in vivo characterization of RO8994 are being reported in a separate communication.

(16) Ding, K.; Lu, Y.; Nikolovska-Coleska, Z.; Qiu, S.; Ding, Y.; Gao, W.; Stuckey, J.; Krajewski, K.; Roller, P. P.; Tomita, Y.; Parrish, D. A.; Deschamps, J. R.; Wang, S. Structure-based design of potent non-peptide MDM2 inhibitors. *J. Am. Chem. Soc.* **2005**, *127* (29), 10130−10131.

(17) Ding, K.; Lu, Y.; Nikolovska-Coleska, Z.; Wang, G.; Qiu, S.; Shangary, S.; Gao, W.; Qin, D.; Stuckey, J.; Krajewski, K.; Roller, P. P.; Wang, S. Structure-based design of spiro-oxindoles as potent, specific small-molecule inhibitors of the MDM2-p53 interaction. *J. Med. Chem.* **2006**, *49* (12), 3432−3435.

(18) Yu, S.; Qin, D.; Shangary, S.; Chen, J.; Wang, G.; Ding, K.; McEachern, D.; Qiu, S.; Nikolovska-Coleska, Z.; Miller, R.; Kang, S.; Yang, D.; Wang, S. Potent and orally active small-molecule inhibitors of the MDM2-p53 interaction. *J. Med. Chem.* **2009**, *52* (24), 7970−7973.

(19) Zhao, Y.; Liu, L.; Sun, W.; Lu, J.; McEachern, D.; Li, X.; Yu, S.; Bernard, D.; Ochsenbein, P.; Ferey, V.; Carry, J.-C.; Deschamps, J. R.; Sun, D.; Wang, S. Diastereomeric spirooxindoles as highly potent and efficacious MDM2 inhibitors. *J. Am. Chem. Soc.* **2013**, *135* (19), 7223−7234.

(20) Zhao, Y.; Yu, S.; Sun, W.; Liu, L.; Lu, J.; McEachern, D.; Shargary, S.; Bernard, D.; Li, X.; Zhao, T.; Zou, P.; Sun, D.; Wang, S. A potent small-molecule inhibitor of the MDM2-p53 interaction (MI-888) achieved complete and durable tumor regression in mice. *J. Med. Chem.* **2013**, *56* (13), 5553−5561.

(21) L., M.; Barreiro, E. J. Bioisosterism: a useful strategy for molecular modification and drug design. *Curr. Med. Chem.* **2005**, *12*, 23−49.

(22) Shu, L.; Li, Z.; Gu, C.; Fishlock, D. Synthesis of a spiroindolinone pyrrolidinecarboxamide MDM2 Antagonist. *Org. Proc. Res. Dev.* **2013**, *17* (2), 247−256.